Magnetic Topology Changes Induced by Lower Hybrid Waves and their Profound Effect on Edge-Localized Modes in the EAST Tokamak

Y. Liang,[1,*] X. Z. Gong,[2] K. F. Gan,[2] E. Gauthier,[3] L. Wang,[2] M. Rack,[1] Y. M. Wang,[2] L. Zeng,[1,2] P. Denner,[1] A. Wingen,[4] B. Lv,[2] B. J. Ding,[2] R. Chen,[2] L. Q. Hu,[2] J. S. Hu,[2] F. K. Liu,[2] Y. X. Jie,[2] J. Pearson,[1] J. P. Qian,[2] J. F. Shan,[2] B. Shen,[2] T. H. Shi,[2] Y. Sun,[2] F. D. Wang,[2] H. Q. Wang,[2] M. Wang,[2] Z. W. Wu,[2] S. B. Zhang,[2] T. Zhang,[2] X. J. Zhang,[2] N. Yan,[2] G. S. Xu,[2] H. Y. Guo,[2] B. N. Wan,[2] J. G. Li,[2] and the EAST team

[1]*Forschungszentrum Jülich GmbH, Association EURATOM-FZ Jülich, Institut für Energie und Klimaforschung Plasmaphysik, Trilateral Euregio Cluster, D-52425 Jülich, Germany*

[2]*Institute of Plasma Physics, Chinese Academy of Sciences, Hefei 230031, China*

[3]*CEA, IRFM, F-13108 Saint-Paul-lez-Durance, France*

[4]*Oak Ridge National Laboratory, P.O. Box 2008, Oak Ridge, Tennessee 37831-6169, USA*

(Received 10 February 2013; published 4 June 2013)

Strong mitigation of edge-localized modes has been observed on Experimental Advanced Superconducting Tokamak, when lower hybrid waves (LHWs) are applied to *H*-mode plasmas with ion cyclotron resonant heating. This has been demonstrated to be due to the formation of helical current filaments flowing along field lines in the scrape-off layer induced by LHW. This leads to the splitting of the outer divertor strike points during LHWs similar to previous observations with resonant magnetic perturbations. The change in the magnetic topology has been qualitatively modeled by considering helical current filaments in a field-line-tracing code.

DOI: 10.1103/PhysRevLett.110.235002 PACS numbers: 52.55.Fa, 52.25.Fi, 52.55.Tn

A great challenge for fusion energy research and technology is to confine a burning plasma while maintaining tolerable steady state and transient heat and particle fluxes on plasma-facing components. When tokamak plasmas operate in a high-confinement (*H*-mode) regime [1], a significant increase in the plasma energy confinement time is observed. However, as a consequence, a steep plasma pressure gradient and an associated increased current density at the plasma edge could exceed a threshold value to drive magnetohydrodynamic instabilities referred to as edge-localized modes (ELMs) [2]. ELMs lead to quasiperiodic expulsions of large amounts of energy and particles from the confined region, which in turn could result in serious damage to plasma-facing components. The next generation fusion machines, like ITER and DEMO, will need a reliable method for controlling or suppressing large ELMs [3].

Resonant magnetic perturbations (RMPs), which change the magnetic topology of the confined plasma, have been applied to completely suppress ELMs in DIII-D [4], or to mitigate ELMs (increase ELM frequency and reduce ELM size) in JET [5], MAST [6], and AUG [7]. Although the physics mechanism is still unclear, experimental results from those different devices demonstrate that the magnetic topology plays a key role in plasma confinement, edge magnetohydrodynamic stability, and interactions between the plasma and the first wall, particularly with the divertor [4,7,8].

To date, in all existing RMP ELM mitigation or suppression experiments, the magnetic perturbations are induced by either in-vessel or external coil systems. In-vessel perturbation coils have been considered and designed for ELM control in ITER. However, in future fusion reactors, like DEMO, in-vessel perturbation coils may not be feasible. Thus, ELM control through actively changing magnetic topology by other mechanisms offers an attractive solution for next generation tokamaks beyond ITER.

Recent results from the Experimental Advanced Superconducting Tokamak (EAST) [9] show that lower hybrid waves (LHWs) provide an effective means to mitigate or suppress ELMs by inducing a profound change in the magnetic topology, similar to the effect previously observed with RMPs [4,5]. In this Letter, the influence of LHWs on the ELM behavior and the heat load distribution on the divertor plates will be presented, along with the experimental observation of LHW-induced nonrotating helical current filaments (HCFs), flowing along the magnetic field lines in the scrape-off layer (SOL). Comparisons are also made between the observed three-dimensional (3D) edge magnetic topology induced by the HCFs and predictions from a field-line-tracing code.

EAST (major and minor radii of 1.85 and 0.45 m, respectively) was built for demonstrating long-pulse stable high-performance *H*-mode plasmas with ITER-like configuration and heating schemes, i.e., with a flexible selection of double null, lower single null (SN), or upper SN poloidal divertor configurations and dominant radio frequency heating. The LHW system [10], operating at 2.45 GHz with an array of 20 (4 columns and 5 rows) waveguide antennas, was installed at the low field side midplane. The maximum output power of the LHW system is 2 MW. It was originally designed for a core plasma

current drive by transferring momentum to the plasma via electron Landau damping with a peak parallel wave refractive index of ~2.1, and can achieve long-pulse H-mode operations with or without additional ion cyclotron resonance heating (ICRH). However, similar to other experiments [11,12], significant LHW power can be lost at the plasma edge, especially in a high-density plasma, due to a complex problem of coupling between fast waves and plasma particles.

The influence of LHW on the characteristics of ELMs has been studied through the modulation of LHW power in an ICRH-dominated H-mode plasma as shown in Fig. 1. In this experiment, the target H-mode plasma with a lower SN configuration was established mainly by ICRH with the input power of 1 MW in a relatively high-density regime after a fresh lithium wall coating. The edge safety factor q_{95} is 3.8 with a toroidal plasma current I_p of 500 kA and a toroidal field B_t of 1.8 T. The bottom triangularity, δ_L, is 0.45. The central line-averaged density, $\langle n_e \rangle$, is $\sim 4.7 \times 10^{19}$ m^{-3}, and the Greenwald fraction is ~0.9. The H factor ($H98y$) obtained during the H-mode phase is ~0.8.

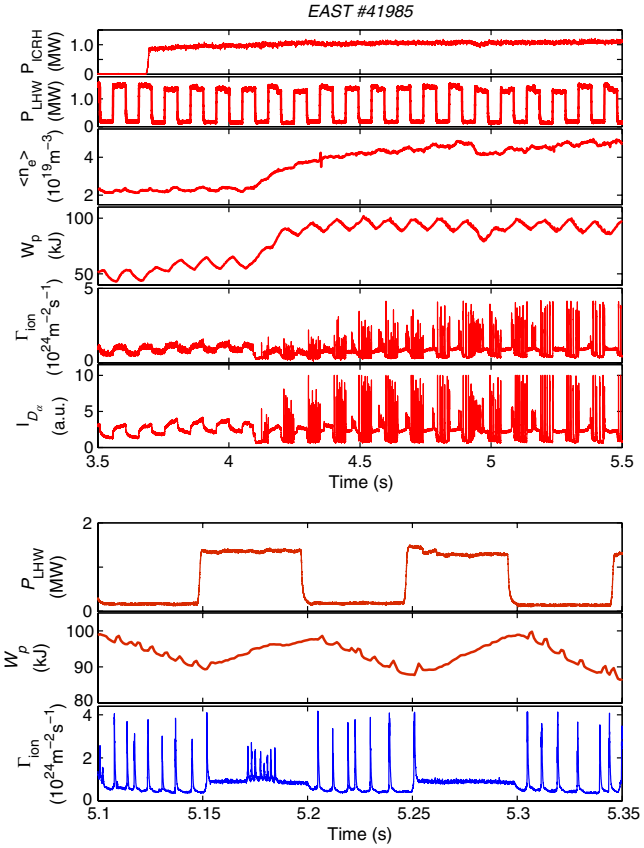

FIG. 1 (color online). Effect of LHW power modulation on ELMs. The time traces from top to bottom are injected power from ICRH and LHW, central line-averaged density, plasma stored energy, peak particle flux, and intensity of D_α emissions in the outer divertor. At the bottom is a focused view of LHW power, stored energy, and peak particle flux in the outer divertor.

The LHW power was set at 1.3 MW and modulated at 10 Hz with a 50% duty cycle. Thus, the duration of the LHW-off phase is 50 ms, which is about half of the energy confinement time. Without LHW, the ELM frequency is fairly regular at ~150 Hz. When LHW is switched on, the ELMs disappear or sporadically appear with higher frequency ~600 Hz as seen in Fig. 1 (lower panel). A significant reduction in the ELM peak particle flux by a factor of ~2 and an increase in the inter-ELM particle flux by a factor of ~2 (but still lower than that in the L-mode phase) have been observed on the divertor plate during the application of LHW. The plasma stored energy W_p was increased by a factor of 2 from ~50 to ~100 kJ once the H mode was established, and varied slightly (within $\pm \sim 5\%$) following the modulation of LHW power. A quick reduction in the divertor ion flux can be clearly seen when the LHW was switched off. This may indicate the LHW power was absorbed not only in the core plasma but also deposited in the SOL.

Five helical radiation belts (HRBs) have been observed in the SOL during the application of LHW in both L-mode and H-mode plasmas on EAST. The number of HRBs is the same as the number of rows of the LHW antenna. Helium gas has been used to make the structure of the HRBs clear without changing its general features. As a typical example, Fig. 2 shows two tangential visible images taken during a helium plasma discharge from different sides of the EAST torus during the application of LHWs. The target plasma ($I_p = 300$ kA, $B_t = 2$ T, $q_{95} \sim 8$) was heated by LHW with a power of 0.7 MW in a double null configuration. The gap between the plasma separatrix and the outer limiter at the midplane is ~8 cm. The HRBs flow through the SOL at the low field side toward both upper and lower outer divertors along field lines in front of the antenna. Modeled SOL field lines, starting at 1 cm away from the original separatrix in front of the LHW antennas, show a good agreement in position and pitch angle with the experimentally observed HRBs.

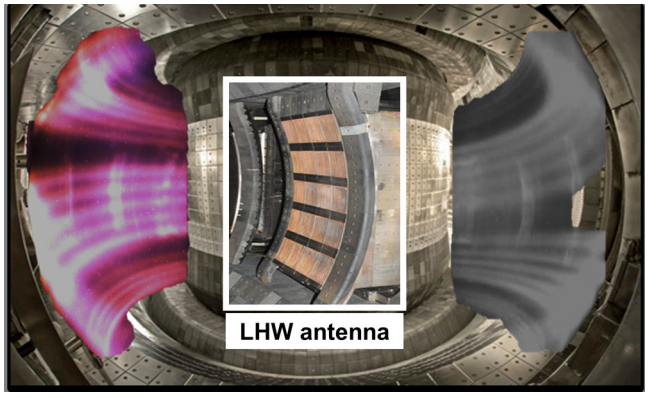

FIG. 2 (color online). Image of helical radiating belts induced by LHW superimposed on the EAST torus chamber. Photo of the LHW antenna on EAST (middle).

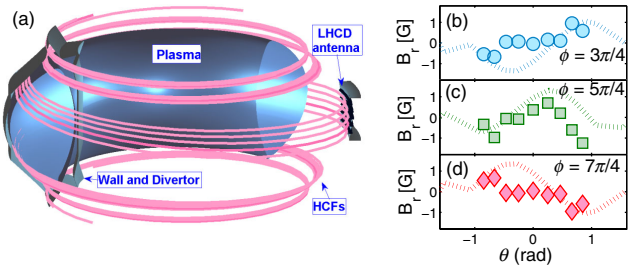

FIG. 3 (color online). (a) The sketch of the HCF modeling and the poloidal profiles of the LHW-induced nonaxisymmetric radial perturbation fields measured at different toroidal sectors with (b) $\phi = 3\pi/4$, (c) $\phi = 5\pi/4$, and (d) $\phi = 7\pi/4$. Here, the poloidal angle θ is defined as starting from the midplane at the low field side and is positive in the clockwise direction. The toroidal angle ϕ starts from the sector containing the LHW antennae in the counter-clockwise direction when viewing the EAST torus from the top. The simulated nonaxisymmetric radial perturbations using the modeled HCFs with a total filament current of 1.3 kA induced by LHW are also plotted.

Magnetic perturbations induced by the currents flowing in these edge helical filament structures (so-called HCFs) have been measured by a set of Mirnov coils during the modulation of LHWs. In this experiment, LHW power was modulated with a square wave from 0 to 1.2 MW, with a repetition rate of 100 Hz and a duty cycle of 50%. The formation of HCF currents was rather quick, i.e., within ~2 ms, which corresponds to the ramp-up time of the LHW. At the start of the LHW, ramp-down HCF currents diffused away within a few ms. The HCF-induced magnetic perturbations are poloidally and toroidally asymmetric, indicating the 3D distortion of the plasma topology. Simulated perturbation fields using the modeled HCFs can reproduce the Mirnov coil signals, as shown in Fig. 3. Here, the HCFs are modeled as currents flowing in the HRBs as seen in Fig. 3(a). The total HCF current can be determined by fitting the simulated perturbation field to the measured one, and is found to be ~1.3 kA in this experiment.

Splitting of the divertor strike points (SP) was observed during the application of LHW with similar effects to those reported for RMPs [13], as manifested in the heat load pattern on the divertor plate; see Fig. 4. The surface temperature on the outer lower divertor plate measured by an infrared (IR) camera during LHW shows a distinct multiple splitting of the original SP. The distance between the secondary and original SPs depends on the toroidal angle, indicating the 3D feature of the magnetic topology caused by LHW. In addition, the splitting of the SP depends on the edge safety factor as well, which was not observed in either Ohmic or ICRH plasmas.

The change in magnetic topology has been qualitatively modeled by considering the HCFs in a field-line-tracing code as shown in Fig. 5. The connection lengths of the magnetic field lines are calculated using an experimental equilibrium superimposed with a perturbation field from the HCFs with a total measured filament current of 1.3 kA.

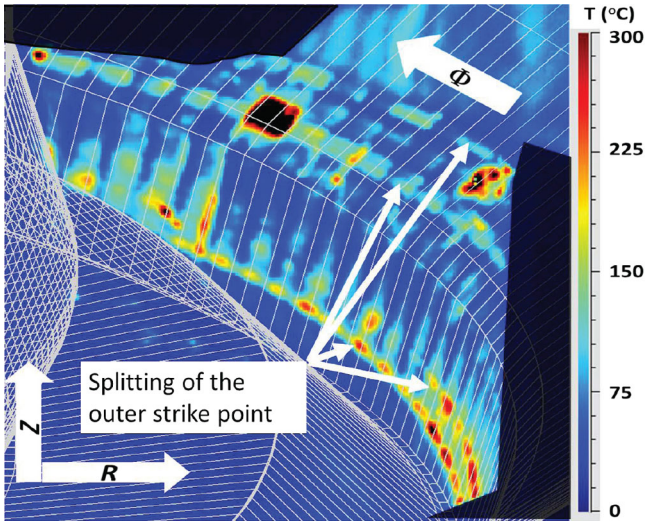

FIG. 4 (color online). IR image of the outer lower divertor plate in a toroidal range of $\varphi = 1.3\pi$–1.5π rad during the application of LHW. Splitting of the original outer SP was shown as a multiple striated heat pattern on the divertor plate. A mesh plot of the wall is superimposed as white lines on the image. The toroidal asymmetry of the SP splitting can be observed.

The fields produced by the HCFs form several lobes of field lines with a long connection length near the X point, which can directly reach the outer divertor plate, resulting in the splitting of the SP, as identified by an IR camera. The calculated results show that strong modifications of the plasma edge depends on the edge safety factor, as well as the amplitude of currents flowing in these filaments.

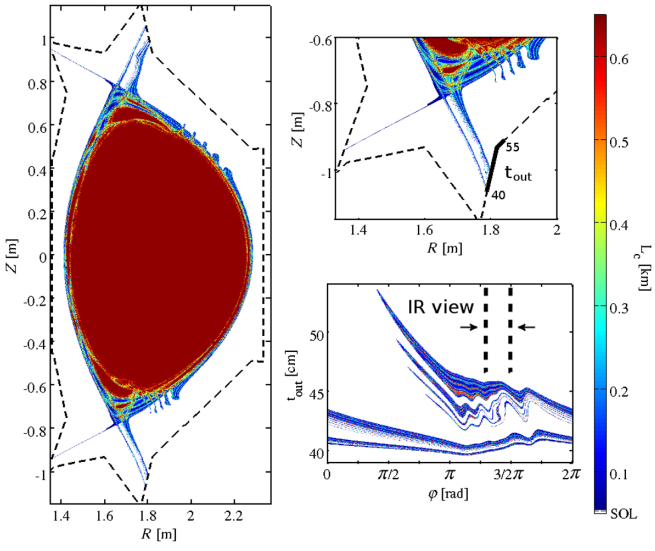

FIG. 5 (color online). Contour of connection length on the full poloidal cross section and expanded view of the bottom divertor region at $\varphi = 1.3\pi$ rad, as well as a calculated footprint on the outer divertor plate as a function of the toroidal angle. Here, the calculation was carried out using the equilibrium reconstructed from the experiment shown in Fig. 4, with the IR viewing region indicated.

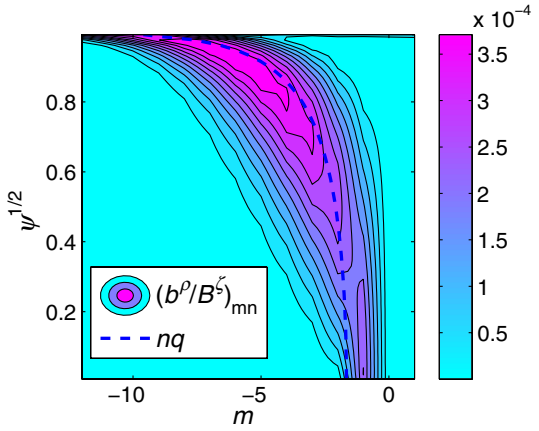

FIG. 6 (color online). Radial component of the $n = 1$ helical mode spectrum calculated with 1 kA HCF current. m is the poloidal mode number, and Ψ is the normalized poloidal flux. The calculation is based on the same equilibrium reconstruction for an EAST pulse shown in Fig. 4. Pitch resonant modes with $m = nq(\Psi)$ are shown by the dashed line.

It should be noted that the HCF model does not take into account the plasma response, and the modeling results can only qualitatively explain the HCF-induced strike point splitting.

Previous experimental results have shown that LHW can produce dithering ELM H modes in SN divertor plasmas on JET [14] and an ELM-free H mode in limiter plasmas on JT-60 [15]. However, the physical mechanism has not been investigated in detail. On EAST, a stationary ELM H mode with mixed type-I and small ELMs can be obtained with an application of stationary LHW power to the ICRH-dominated plasmas in a relatively low-density regime ($n_e/n^{\mathrm{GW}} < 0.5$). Here, n^{GW} is the Greenwald-density limit. By decreasing the ratio of ICRH to LHW power and increasing plasma density, a stationary small ELM H-mode regime has been achieved and sustained for 32 s. The new evidence of HCFs induced by the LHW and its effects on the magnetic topology provide a possible explanation for why LHW mitigates or suppresses ELMs and induces a significant change in the heat load pattern on the divertor plate. For an understanding of the physical mechanism behind this, the dependences of LHW ELM mitigation on (i) the lithium wall coating [16], (ii) plasma pedestal collisionality, and (iii) q_{95} will be performed in future EAST experiments.

Because of the geometric effect of the LHW antenna, the perturbation fields induced by the HCFs are dominated by the $n = 1$ components, where n is the toroidal mode number. The magnetic perturbation spectrum calculated based on the experimental parameters indicates a good resonant feature, whereby the plasma edge resonant surfaces are well aligned on the ridge of the spectrum as shown in Fig. 6. In addition, the HCF-induced magnetic perturbations are located more at the plasma edge, without significantly affecting the plasma core. This is mainly because the HCFs flow along the magnetic field lines in the SOL; thus, the helicity of the HCFs always closely fits the pitch of the edge field lines for whatever the plasma edge safety factor is.

It is to be mentioned that the currents in the SOL induced by LHW have been observed on several devices [11,12], however, the physical mechanism is still unclear. On Alcator C-Mod, the direction of the currents in the SOL did not change when the direction of LHW injection was reversed [11]. The estimated current in the SOL can be up to ~20 kA with a LHW power of 850 kW in a high-density regime on Alcator C-Mod, while the poloidally integrated total HCF current is ~7 kA with a LHW power of 1.3 MW on EAST. A simulation using the GENRAY-CQL3D code package [11] with a two-dimensional SOL model including the effects of collisional damping shows that about 10% of LHW power can be deposited in the SOL in the high-density plasmas on EAST. The experimentally observed currents in the SOL are far too large to be explained by direct current drive via collisional absorption of the LHW [12]. Note, however, that the absorption of LHW in the SOL could contribute to an increase in the ionization rate for neutrals in the divertor region, thus enhancing the thermoelectric current flowing along the SOL field lines from the hotter, less dense divertor plate to the colder, denser divertor plate.

On EAST, preliminary results show that the amplitude of the HCF current increases with an increase in either the LHW power or the plasma density. However, the radial location of the HCFs mostly stays near the separatrix in the SOL, where the connection length of field lines is much longer than the electron mean-free path. To achieve active control of the ELMs and heat load distribution on the divertor plates by LHW, parametric dependance of the HCF currents will be further investigated on EAST.

In summary, strong influence of LHWs on ELMs has been demonstrated on EAST, showing that the ELMs disappeared or sporadically appeared with increased frequency from ~150 to ~600 Hz when LHW was applied. LHW appears to induce a profound change in the magnetic topology by driving the nonrotating HCFs flowing along the magnetic field lines in the SOL. This leads to the splitting of the divertor SP with effects similar to those produced by RMPs. The observed change in topology is well reproduced by considering the HCFs in a field-line-tracing code. This offers a new attractive means to optimize the heat load distribution on the divertor plates and to suppress or mitigate the large transit peak heat and particle loads due to ELMs for the next-step fusion reactors (ITER and DEMO).

This work was supported by the National Magnetic Confinement Fusion Science Program of China under Contracts No. 2013GB106003 and No. 2011GB107001. Support from the Helmholtz Association in the frame of the Helmholtz-University Young Investigators Group VH-NG-410 is gratefully acknowledged.

*y.liang@fz-juelich.de; www.fz-juelich.de

[1] F. Wagner *et al.*, Phys. Rev. Lett. **49**, 1408 (1982).
[2] J. W. Connor, Plasma Phys. Controlled Fusion **40**, 531 (1998).
[3] ITER Physics Basis Editors, ITER Physics Expert Group Chairs and Co-Chairs, and ITER Joint Central Team and Physics Integration Unit, Nucl. Fusion **39**, 2137 (1999).
[4] T. E. Evans *et al.*, Nat. Phys. **2**, 419 (2006).
[5] Y. Liang *et al.*, Phys. Rev. Lett. **98**, 265004 (2007).
[6] A. Kirk *et al.*, Nucl. Fusion **50**, 034008 (2010).
[7] W. Suttrop *et al.*, Phys. Rev. Lett. **106**, 225004 (2011).
[8] Y. Liang, C. G. Gimblett, P. K. Browning, P. Devoy, H. R. Koslowski, S. Jachmich, Y. Sun, and C. Wiegmann, Phys. Rev. Lett. **105**, 065001 (2010).
[9] J. G. Li and B. N. Wan, Nucl. Fusion **51**, 094007 (2011).
[10] B. J. Ding *et al.*, Phys. Plasmas **18**, 082510 (2011).
[11] G. M. Wallace *et al.*, Phys. Plasmas **17**, 082508 (2010).
[12] R. McWilliams, E. J. Valeo, R. W. Motley, W. M. Hooke, and L. Olson, Phys. Rev. Lett. **44**, 245 (1980).
[13] D. M. Harting, Y. Liang, S. Jachmich, R. Koslowski, G. Arnoux, S. Devaux, T. Eich, E. Nardon, D. Reiter, and H. Thomsen, Nucl. Fusion **52**, 054009 (2012).
[14] F. X. Söldner *et al.*, Europhys. Conf. Abstr. **22**, 1190 (1998).
[15] S. Tsuji *et al.*, Phys. Rev. Lett. **64**, 1023 (1990).
[16] J. M. Canik *et al.*, Nucl. Fusion **50**, 034012 (2010).